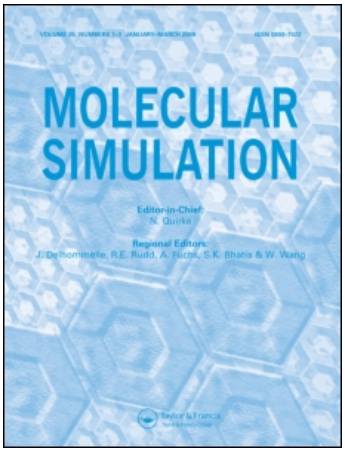

Molecular Simulation
Publication details, including instructions for authors and subscription information:
http://www.informaworld.com/smpp/title~content=t713644482

Simulation of Lamellar Phase Transitions in Block Copolymers and Surfactants

R. G. Larson[a]
[a] AT & T Bell Laboratories, Murray Hill, New Jersey

To cite this Article Larson, R. G.(1994) 'Simulation of Lamellar Phase Transitions in Block Copolymers and Surfactants', Molecular Simulation, 13: 4, 321 — 345
To link to this Article: DOI: 10.1080/08927029408021996
URL: http://dx.doi.org/10.1080/08927029408021996

Molecular Simulation, 1994, Vol. 13, pp. 321-345
Reprints available directly from the publisher
Photocopying permitted by license only

SIMULATION OF LAMELLAR PHASE TRANSITIONS IN BLOCK COPOLYMERS AND SURFACTANTS

R. G. LARSON

AT & T Bell Laboratories, Murray Hill, New Jersey 07974

(Received October 1993, accepted April 1994)

Simulations of the lamellar phase transitions of symmetric amphiphilic chains are carried out on a cubic lattice, with the amphiphilic chain length N varied from 6 to 48 lattice sites, corresponding to lengths ranging from surfactants to short block copolymers. We find that the effective interaction energy parameter χN (which incorporates the effect of added solvant) at which the transition from the lamellar ordered state to the disordered state occurs is roughly equal to 18–21. While this result is consistent with an extrapolation of the Fredrickson-Helfand weak-segragation theory to N values in the range of the simulations, the amplitude of the sinusoidal compositional wave in the ordered state near the transition is large for all N studied, in disagreement with the weak segregation theories. Thus, for values of N up to 48, the transition occurs in a "moderate," rather than weak-segregation regime. Near the disordering transition, fluctuating "bridge" or "hole" defects in the lamellae spontaneously appear; with heating these proliferate and lead to the disordering transition. These fluctuating bridges might help explain anomalous diffusion and rheological behavior observed near the disordering transition. We also find that in the ordered state near the transition, the orientational order parameter, which is proportional to the intrinsic birefringence, falls rapidly with increasing N, roughly as $1.5\,N^{-2}$.

KEY WORDS: Lamellar phase transitions, block copolymers, surfactants.

I INTRODUCTION

Linear diblock copolymers, which are composed of two chemically distinct polymers that are covalently bonded together, exhibit phase behavior and microdomain morphologies that are similar in many respects to those of small-molecule surfactants. Both surfactant and block-copolymer amphiphiles, in the neat state, or when mixed with solvents or homopolymers, can form spherical or cylindrical micelles, hexagonal phases, lamellar phases, and ordered cubic and non-cubic bicontinuous intermediate phases [1–9]. In both types of system, the entropic and energetic factors that govern the selection of the equilibrium microdomain pattern include the repulsive energies that tend to separate the two dissimilar "blocks" or moieties, the range of conformational states available to the amphiphilic molecule (e.g., its flexibility), the volume fractions of each block, as well as that of added solvents, the possible presence of ionic species, and, of course, the temperature. In fact, one might think of ordinary surfactants as very short block copolymers. Of course, there are likely to be important differences between block copolymers and small-molecule surfactants, owing in part to the great size difference between the two molecules.

Theories of the phase behavior and molecular organization of ordered *high molecular-weight* block copolymers have been developed by numerous authors [10–17]. These theories take advantage of the Gaussian or near-Gaussian statistical properties of large flexible molecules, and use mean-field or weak-fluctuation approximations. Such theories are directed at either of two regimes, controlled by the value of the product χN, where N is the degree of polymerization and χ is the usual Flory interaction energy parameter, which for most block copolymers is a decreasing function of temperature. At high χN, one is in the *strong segregation* regime, where the chemically distinct blocks are largely unmixed from each other except at rather sharp interfaces. For strongly segregated blocks, fluctuation effects are thought to be small, and mean-field theories are rather accurate. In the *weak segregation regime* at low or modest χN, the blocks are only modestly segregated, and compositional gradients are small. A mean-field theory for weakly segregated block copolymers was developed by Leibler [12] which predicts a lamellar order-disorder transition (ODT) for symmetric diblock copolymers at $\chi N = (\chi N)_{ODT} = 10.5$. In the ordered state close to this transition, the Leibler theory predicts that the lamellar structure consists of an undamped stationary one-dimensional sinusoidal compositional wave, whose amplitude passes continuously to zero as the disordering temperature is approached.

However, the effect of fluctuations is neglected in the Leibler treatment. As Fredrickson and Helfand have emphasized [13], fluctuations become important as the disordering transition is approached from the ordered state or from the disordered state. The dominant fluctuations are quasi-sinusoidal composition waves, with wavelengths similar to that of the stationary wave. Near the transition, in the weak-segregation limit, the fluctuations are damped slowly in time and space; they are thus coherent over a large, yet finite, number of wavelengths. Furthermore, these waves are *randomly oriented* in space, so that the compositional pattern near $(\chi N)_{ODT}$ consists of a superposition of such waves oriented at all angles. These slow, fluctuating, waves are superposed on the infinitely coherent stationary wave if $\chi N > (\chi N)_{ODT}$, and on the isotropic state if $\chi N < (\chi N)_{ODT}$. Fredrickson and Helfand (FH) showed that these compositional fluctuations shift $(\chi N)_{ODT}$ upward and change the transition from continuous to discontinuous, or first order. Using a free energy expansion of Brazovskii [18] valid for small-amplitude fluctuations, they computed the magnitude of the compositional fluctuations and the degree of shift in $(\chi N)_{ODT}$ caused by fluctuations as a function of the block copolymer polymerization index N. They found that the effects of fluctuations become weaker at higher N, and the Leibler mean-field result is recovered asymptotically as $N \to \infty$. Omitted from the HF theory are *chain stretching effects* – i.e., deviations from random-flight statistics – that are produced becuase even in the disordered state finite-amplitude composition fluctuations provide an energy inducement for the two distinct blocks to separate from each other. The effects of chain stretching were included in a more recent theory by Barrat and Fredrickson [14]; this theory predicts a smaller fluctuation-induced shift in $(\chi N)_{ODT}$ and a wider lamellar spacing than does the FH theory.

The FH and BF weak-fluctuation theories are perturbative; they are in principle only valid for high molecular-weight polymers for which fluctuation effects are modest and deviations from the Leibler mean-field theory are small. However, as the molecular weight of the diblock copolymer becomes smaller, the fluctuation effects are expected

to become ever more important, and one would expect weak segregation theories to fail well before the blocks become as short as they are in surfactants. Since the phase behavior and molecular organization of low molecular weight block copolymers are receiving increasing attention, in part because of their possible similarity to surfactant amphiphiles, it would be of interest to look for possible deviations from weak-fluctuation theories as N becomes smaller.

II LATTICE MODEL

While it is useful to compare experimentally the behavior of small-molecule amphiphiles with polymeric ones, it can be difficult by experiments alone to determine the origin of any differences one might observe between the two types of amphiphilic systems. For this reason, computer simulations are useful. The properties of the "molecules" used in computer simulations can be controlled precisely, and many limitations of experiments, such as those on chemical stability and on the available temperature range, can be avoided. Also, in computer simulations, all molecular or structural details of the phases formed can readily be calculated. Of course, computer simulations are limited in the size of the system to which they can be applied and in the time that can be allowed for equilibration. But we are here especially interested in examining short diblock chains, with a range of lengths that encompasses both ordinary surfactants and short block copolymers, and for these, computer simulations are well suited. Thus, computer simulations can provide a useful bridge between experimental studies of short amphiphiles and weak-segregation theories of block copolymers.

We shall use computer simulations to examine the effect of amphiphile length on the transition from the isotropic to lamellar phase, and on the molecular organization of the lamellar phase. We will compare the behavior of short amphiphiles, which can be thought of as model surfactants, with longer amphiphiles, which can be considered short model diblock copolymers. While diblock copolymers are often called "A-B" block copolymers, where "A" and "B" represent the two different polymeric blocks, in linear surfactants the two distinct chemical moieties are typically called the "head," which is usually hydrophilic, and the "tail," which is hydrophobic. For convenience, we will use a unified terminology in which "head" can represent either the hydrophilic group of a surfactant or one of the blocks, say, block A of a copolymer. We similarly generalize the term "tail."

To examine systematically the effect of amphiphile length on the ordering transitions between the disordered state and the lamellar or smectic state, we apply a Monte Carlo simulation procedure to a simply Flory-type lattice model [19–20]. For reasons to be discussed shortly, we shall include a modest volume fraction of solvent molecules in our simulation. The solvent molecules are of two types; one of them, which we call "water," is taken to be chemically identical to the head group (or block "A"); the other, which we call "oil," is chemically identical to the tail group (or block "B"). These oil and water solvent molecules occupy single sites of a simple cubic lattice. The expected directional bias of the cubic lattice is reduced by allowing a site to interact pairwise additively with all $z = 26$ nearest, face-diagonal, and body-diagonal nearest neighbors, all with equal strength. The surfactant or block-copolymer molecule occupies a sequence of lattice

sites connected along any of these same 26 directions. The amphiphile sites are occupied by either head (water-loving) or tail (oil-loving) units. The head and tail units interact with their neighbors just as do water and oil units, respectively, so that there is a single dimensionless interaction energy parameter w, which is the interaction energy per oil/water contact, divided by k_BT. The nomenclature H_iT_j defines a surfactant that consists of a string of i head units attached to j tail units. The usual periodic boundary conditions are used.

Rearrangements of the molecules take place by oil/water interchanges, and by kink and repetation motions of the amphiphile, as described elsewhere [19]. To prepare equilibrium structures, an initially random arrangement of molecules at infinite temperature ($w = 0$) is cooled slowly by increasing w in small increments, until an ordered pattern forms. Near the ordering transition, the size of the increment, Δw, was chosen to be small, and scaled inversely with the length of the amphiphile so that the ratio $\Delta w/w_0 \approx 0.02$ was kept roughly independent of N. Here w_0 is w at the ordering transition. To show that the pattern is that of an equilibrium bulk state, runs are repeated on lattices of different sizes and at different cooling rates. As described in earlier publications [19], the number of attempted Monte Carlo moves that are needed to achieve an equilibrium pattern varies with the size of the box L, the inverse dimensionless temperature w, and the particular surfactant, its volume fraction, and the volume fractions of solvent, oil or water. During simulations of cooling or heating, the averaged system energy $\langle E \rangle$ is monitored, where E is the energy per lattice site divided by w. Hence $\langle E \rangle$ is the average number of unfavorable contacts per lattice site. Increments of temperature are taken only after $\langle E \rangle$, averaged over a run of around 10^4 attempted MC moves per lattice site, stabilizes at a value that is constant to within around ± 0.005, which is very small compared to the change in $\langle E \rangle$ that occurs when w is incremented. Near ordering or disordering transitions, drifts in $\langle E \rangle$ greater than 0.005 were often detected. In these cases, equilibration times were extended to as long as needed to bring the drift within the above criterion; this required runs as long as 10^5 attempted Monte Carlo moves per site.

The longest amphiphilic molecule whose phase behavior we have studied is $H_{24}T_{24}$, a short "block copolymer" consisting of 24 head units and 24 tail units, for a total of $N = 48$ units. If we consider each unit of this "block copolymer" to correspond to one link of a "freely-jointed" chain, then, using the conventional statistical treatment of polymer molecules, a polystyrene molecule with 48 such units would have a molecular weight of around 48,000, for a polyisoprene molecule the molecular weight would be 15,000, and for polyethylene, it would be around 4,500 [21]. Thus, although the longest amphiphiles considered here represent short block copolymers, they are nevertheless within the range of some recent experimental studies [22–24]. At the other extreme, the shortest model chain we consider is H_3T_3. While the aspect ratio of this "molecule," when fully stretched, is comparable to some typical small-molecule surfactants, the lattice chain has more conformational freedom than do the experimental ones. For example, to have the same flexibility as a model chain with 3 freely rotating links, an alkane chain would have contain around 20 carbon atoms in the backbone, and would have an aspect ratio of around 20 to 1. Thus, the short amphiphiles used in the simulation here are more flexible than most real surfactant molecules. However, the model can readily be adjusted to restrict the number of conformations available to an

amphiphile, and so make it much stiffer; the effect of increased molecular stiffness will be considered in the future.

From our molecular simulations, we can extract the location of the phase transition, the orientational and compositional order parameters of the lamellar state, and details about the equilibrium molecular configurations in the various ordered and disordered states that are spontaneously produced by the simulations. Of particular interest is the degree to which departures from weak-segregation/weak-fluctuation theories are observed with decreasing amphiphile size. Also of interest is the degree to which the amphiphiles depart from their high-temperature random configurations when the solutions containing them are cooled into ordered states.

III CHARACTERIZATION OF EQUILIBRIUM PHASES

A Chain configurations

To characterize the distribution of molecular configurations in an equilibrium phase, we define $Q(r^2)$ to be the probability that the ends of amphiphilic chain are separated by a squared distance of r^2 lattice sites. Thus if i_x, i_y, and i_z are the distances of separation between ends of the amphiphile in each of the three directions on the lattice, then $Q(r^2)$ is the probability that $i_x^2 + i_y^2 + i_z^2 = r^2$. After equilibrating the system, this probability $Q(r^2)$ is computed by finding the numbers of chains on the lattice whose ends are separated by a squared distance r^2, and then dividing by the total number of chains. Statistical fluctuations are averaged out by continuing the Monte Carlo simulation after equilibration until a significantly different realization of the equilibrium system is achieved. The required statistical quantities are then computed again and averaged into the old quantities. This process is repeated roughly one hundred times, so that statistical noise is small even for rare chain configurations.

An artifact of the lattice model is that some squared distances are not possible, for instance $i^2 = 7$ is impossible, since there is no sum of three squared integers that can equal 7. To minimize the artificiality of our results, we therefore average over values of r^2 by lumping the probabilities $Q(r^2)$ for values of r^2 that are *not* perfect squares with the probabilities for neighboring values of r^2 that *are* perfect squares of an integer. Thus for $r^2 = 10$, ($r = 3.16$), we divide $Q(r^2 = 10)$ into two parts; one part is lumped with the probability for 3^2 and the other part that for 4^2. The portion of $Q(r^2 = 10)$ lumped with $Q(r^2 = 3^2)$ should be much larger than that lumped with $Q(r^2 = 4^2)$, since 3 is much closer to $\sqrt{10}$ than is 4. We also want to preserve the condition that the sum of the probabilities is unity, and that mean square distances computed using these lumped probabilities are not affected by the lumping procedure. Thus we wish to define a new lumped probability $P(i^2)$ that satisfies the following conditions:

$$\sum_{i=\text{integer}} P(i^2) = 1; \quad \sum_{i=\text{integer}} i^2 P(i^2) = \sum_{r^2=\text{integer}} r^2 Q(r^2). \tag{1}$$

These conditions determine the new lumped probability distribution function $P(i^2)$ as

$$P(i^2) \equiv \sum_{r^2=(i-1)^2+1}^{i^2-1} \frac{r^2-(i-1)^2}{i^2-(i-1)^2} Q(r^2) + \sum_{r^2=i^2}^{(i+1)^2-1} \frac{(i+1)^2-r^2}{(i+1)^2-i^2} Q(r^2) \tag{2}$$

where $P(i^2)$ is only defined for integer values of i.

While $P(i^2)$ characterizes the distribution of end-to-end lengths of the entire molecule, we can also characterize the conformation distributions of the head and tail portions of the molecule. We do this by defining the probabilities $P_H(i_H^2)$ and $P_T(i_T^2)$, where P_H(or P_T) is defined the same way as P, but with i_H(or i_T) defined as the end-to-end distance of separation of one end of the head (or tail) from the other. Gross measures of the degree of stretch of the chain, the head group, and the tail group, are defined respectively by

$$R^2 \equiv \sum_{i=\text{integer}} i^2 P(i^2); \quad R_H^2 \equiv \sum_{i=\text{integer}} i^2 P_H(i^2); \quad R_T^2 = \sum_{i=\text{integer}} i^2 P_T(i^2) \tag{3}$$

B Orientational and Compositional Order Parameters

We shall also compute the *orientational order parameter* p_2 from our model for the various lamellar phases. To do this, we first compute an orientation tensor p_{ij}:

$$p_{ij} = \frac{\langle b_i b_j \rangle}{\langle b^2 \rangle} \tag{4}$$

In the above, b_i is the length of an amphiphile bond projected on direction i, with $i = 1$, 2, or 3; b_j is similarly defined with $j = 1$, 2 of 3. Since two connected units of an amphiphile are either nearest neighbors, face-diagonal nearest neighbors, or body-diagonal nearest neighbors, b_i is either zero or one. The braces "$\langle\ \rangle$" in equation (4) represent an ensemble average over all amphiphile-amphiphile bonds. This average is computed by averaging $b_i b_j$ over all amphiphile bonds on a given realization of the equilibrated system, and then averaging over multiple realizations produced by an extended Monte Carlo run, as discussed above. For our lattice model, each unit on the chain can be connected to a neighboring unit via any one of 26 possible bonds; 6 of these are nearest-neighbor bonds of length 1 unit cell, 12 are face-diagonal bonds of length $\sqrt{2}$, and 8 are body-diagonal bonds of length $\sqrt{3}$. If each of these 26 bonds occur with equal probability, then the mean square bond length $\langle b^2 \rangle$ is given by $(6 + 12 \times 2 + 8 \times 3)/26 = 2.08$.

Our computer simulations show that in an isotropic phase, the orientation tensor obtained using equation (4) gives, to within statistical noise, the expected result

$$p_{ij} = \frac{1}{3}\delta_{ij} \tag{5}$$

where δ_{ij} is the Kronecker delta.

When the lamellar phase forms, p_{ij} becomes anisotropic; this anisotropy reflects an orientational bias in the segments induced by the lamellar phase. It is convenient to choose a box size for which the lamellae are parallel to a face of the box, say the x–y face. In this case, we expect the orientation tensor to be diagonal; and we expect that $p_{zz} > p_{yy} = p_{xx}$. The orientational order parameter p_2 can then be defined as

$$p_2 \equiv p_{zz} - \frac{1}{2}(p_{xx} + p_{yy}) \tag{6}$$

In equation (6), slightly improved statistical averaging is obtained by subtracting the average of p_{xx} and p_{yy}, rather than just p_{xx} or p_{yy}, from p_{zz}.

If the lamellae are not oriented parallel to a side of the simulation box, we can use a rotation matrix Q_{ki} to rotate the orientation tensor into a frame in which the lamellae are parallel to the x–y plane:

$$\hat{p}_{kl} = Q_{ik}^T p_{ij} Q_{jl} \tag{7}$$

where $\hat{p}_{kl}$ is the orientation tensor in the rotated frame. This rotation matrix should diagonalize the orientation matrix, if the orientation tensor is uniaxial, which will be the case *if lattice bias effects are negligible.* As will be discussed in section IV-B, we find, however, that because of lattice bias, there is *for short chains* a modest departure from uniaxiality when the lamellae are not parallel to a face of the box, and the rotation equation (7) does not reduce the off-diagonal components of the orientation matrix to zero; neither does it render $\hat{p}_{xx}$ equal $\hat{p}_{yy}$. Also, the order parameter computed from equation (6) with p replaced by $\hat{p}$ is somewhat higher than that obtained for lamellae that are parallel to a face of the box. For long amphiphiles, this lattice bias effect seems to disappear. It is significant that p_2 is the only quantity for which we have observed significant lattice bias artifacts in our simulations.

The orientational order parameter p_2 is proportional to the *intrinsic birefringence* of the lamellar phase. To compute the *form birefringence* from the lattice computations, we need to obtain the compositional order parameter. We define the average compositional pattern as $\langle C_i(x, y, z)\rangle$, where x, y, and z stand for the lattice coordinates, and i can stand for head, tail, oil or water. The braces represent an average over several realizations generated during an extended Monte Carlo run. From $\langle C_i(x, y, z)\rangle$, one dimensional composition profiles can be generated by averaging over the two directions perpendicular to the direction of interest. Thus, if the pattern contains lamellae oriented parallel to the x–y plane, the average lamellar compositional wave is obtained as

$$\langle C_i(z)\rangle \equiv \frac{1}{L^2}\sum_{x,y}\langle C_i(x, y, z)\rangle \tag{8}$$

where L is the linear dimension of the cubic lattice. If a sine function can be fit to $\langle C_i(z)\rangle$, then the amplitude of this sine function, relative to the maximum amplitude possible, can be used as the definition of the compositional order parameter.

IV RESULTS

The simple Flory-type lattice model allows us to examine the relationship between short amphiphiles, characteristic of surfactants, and long amphiphiles, characteristic of block copolymers. In particular, we consider in detail the transitions from disordered to lamellar phases in solutions of symmetric amphiphiles H_iT_i, with $i = 3 - 24$. The concentration C_A of amphiphile is taken to be less than unity; the lattice sites not occupied by amphiphile are occupied by solvent units, namely oil and water, with equal amounts of each. We include solvent because the reptation moves mentioned in section II are only possible when the lattice contains either vacant sites or single-site solvent molecules. Although the kink-like motions can occur even when solvent is absent – and therefore it is possible to equilibrate the system without reptation moves – equilibr-

ation is much faster when reptation is possible, especially for the long molecules considered here. Since we will be considering long runs, we include in most cases a significant amount of solvent, namely 40% by volume. However, by considering cases with as little as 10% solvent, we show later that the effect of the solvent on the phase transitions can be accounted for.

A Transition temperatures and lamellar spacings

As described in section II, initially disordered systems at $w = 0$ are "cooled" by raising w in small increments, and equilibrating between increment. Figure 1a,b shows a slice of a $40 \times 40 \times 40$ lattice containing 60% H_3T_3, 20% water and 20% oil, with

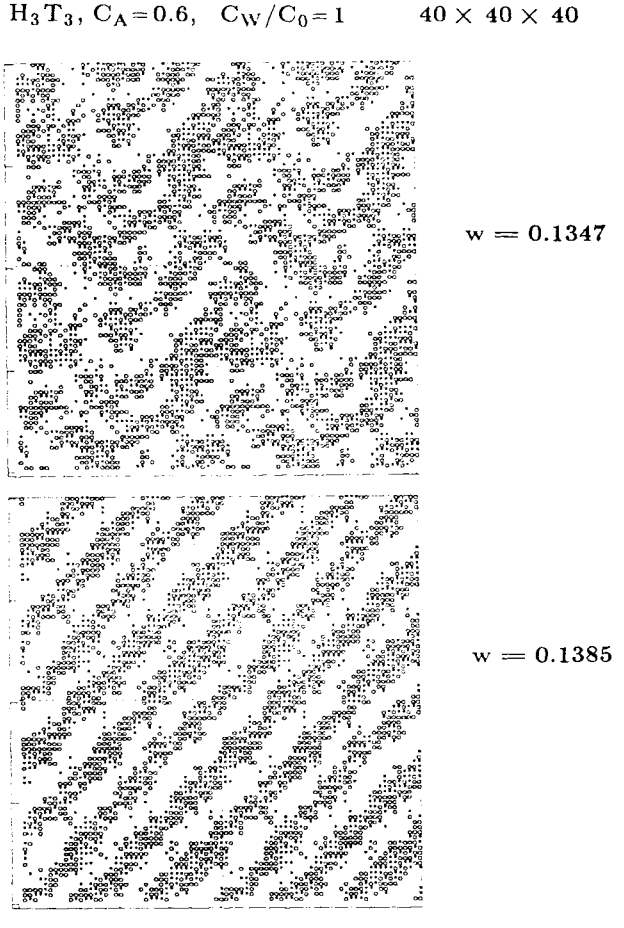

Figure 1 Slices of a $40 \times 40 \times 40$ system containing 60% H_3T_3 with an oil/water ratio of unity. The circles represent tail units; the asterisks are oil units. Except where otherwise noted, these and succeeding images contain four periodic copies of the simulated system, which is enclosed in dashed lines. **a** The disordered state equilibrated at $w = 0.1347$; **b** The ordered state obtained by cooling the disordered state shown in **a** to $w = 0.1385$, and equilibrating.

$w = 0.1347$ and $w = 0.1385$, which are respectively just below and just above w_0. Note the abrupt transition from a disordered "spinodal-like" pattern at $w = 0.1347$ to a lamellar state at $w = 0.1385$. We show in Figure 2a,b the corresponding disordered and ordered patterns for 60% $H_{24}T_{24}$ in 20% oil and 20% water. The orientation of the lamellae on the lattice is controlled by the lattice size; the lamellae select an orientation in which the lamellar spacing is close to that of a bulk system [20]. It was shown elsewhere [20] that for boxes large enough to contain at least two lamellar repeat spacings, the lamellar spacing selected varies by no more than about 5% as one changes the box size. If the lattice box size is chosen appropriately, the lamellae self assemble with their orientation parallel to a face of the box; a fact that we exploit later.

Once ordering is achieved, we increase the effective "temperature" by decreasing w, again in small increments, and re-equilibrate the system between each increment in w. Eventually, at $w = w_d$, a *disordering* transition is reached at which the lamellar state "melts" back to a disordered state. Table 1 compiles the values of w_0 and w_d for a series

$H_{24}T_{24}$, $C_A = 0.60$, $C_W/C_0 = 1$, $60 \times 60 \times 60$

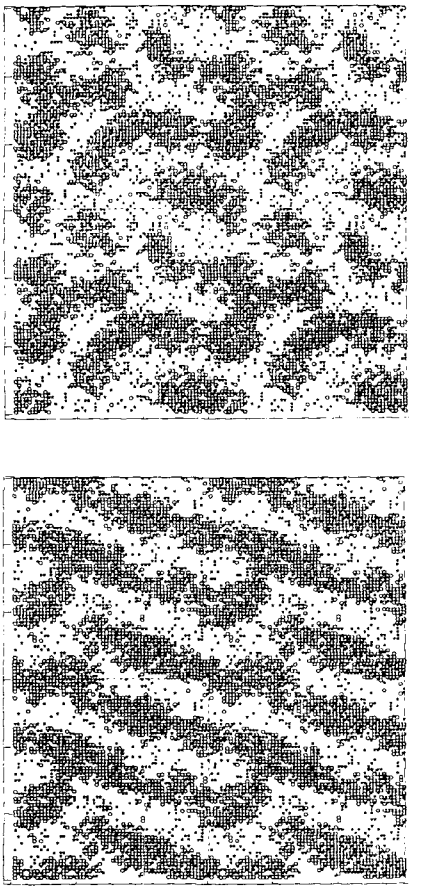

Figure 2 The same as in Fig. 1, except the lattice size is $60 \times 60 \times 60$, and the amphiphile is $H_{24}T_{24}$.

Table 1 Lamellar transitions for $C_A = 0.60$, O/W = 1.

	Box size	C_A	w_0	w_d	$1 - \frac{w_d}{w_0}$	*Spacing d*	$d/R_{g,0}$
H_3T_3	$40 \times 40 \times 40$	0.6	0.1370	0.1340	0.02	8.53	6.48
H_4T_4	$40 \times 40 \times 40$	0.6	0.1120	0.1080	0.04	9.43	6.06
H_6T_6	$40 \times 40 \times 40$	0.6	0.0870	0.0820	0.06	11.09	5.68
H_8T_8	$40 \times 40 \times 40$	0.6	0.0730	0.0660	0.10	12.65	5.55
$H_{12}T_{12}$	$40 \times 40 \times 40$	0.6	0.0530	0.0485	0.08	14.14	5.01
$H_{24}T_{24}$	$60 \times 60 \times 60$	0.6	0.0335	0.0275	0.18	18.97	4.70
$H_{24}T_{24}$	$38 \times 38 \times 38$	0.6	0.0310	0.0265	0.15	19.00	4.71

of symmetric-amphiphile solutions. The lamellar spacing d at $w = w_0$ is also tabulated. Not surprisingly, with increasing amphiphile length N, the transition values of w_0 and w_d decrease, and the spacing d decreases. Note that there are two entries for $H_{24}T_{24}$; from the lamellar spacing on the $60 \times 60 \times 60$ lattice we inferred that the lamellae would be parallel to a face of a $38 \times 38 \times 38$ lattice, and this indeed proved to be the case.

To compare our simulation results with weak segregation theories, we will need to define the Flory "chi" parameter for our lattice model. In the Flory model, χ is the energetic cost per monomer of placing an amphiphile head group into an environment containing only tail or oil units. Since each unit on the amphiphile interacts with $z = 26$ neighbors, we might expect $\chi = zw$. However, as noted by Guggenheim, and discussed by Sariban and Binder [25], each monomer, except for those at the ends, is bonded to 2 of its neighbors, and thus really has no more than $z - 2$ neighbors that are not bonded to the same chain. Since the chain can fold back on itself, even some of the remaining $z - 2$ neighbors are likely to be occupied by units from the same chain. The weak segregation theories to which we want to compare our simulation results do not account for these self interactions, and so, in principle, they should be accounted for by using an effective coordination number z_{eff}. Fortunately, in our lattice model, the coordination number is high, and so in relative terms the corrections are small. Nevertheless, for a given amphiphile, composition, and w value, a correction to the coordination number can be computed from the simulations as follows. First, we compute the average number z_{self} of self-interacting neighbors to an amphiphile unit, i.e., the average number of neighbors that are on the same chain, whether bonded directly or indirectly to the given unit. This turns out to be around $z \approx 4$, depending only slightly on the amphiphile. It turns out that for long chains, say $N = 48$, most (i.e., 90%) of these self-interactions are between like units, because each block is long enough that the unlike units are typically displaced far enough away from a given unit to rarely interact with it. Thus, most of the $z_{\text{self}} = 4$ self-interactions per monomer are "excess" interactions that must be subtracted from z to obtain z_{eff}, so that for $N = 48$, $z_{\text{eff}} \approx z - z_{\text{self}} \approx z - 4$. However, for short chains, especially for $N = 6$, unlike units on the same chain are not far from each other, and computations show that the probability that a self-interaction is repulsive is almost the same as the probability that a non-self-interaction is repulsive. Thus, for $N = 6$, z need not be corrected, and $z_{\text{eff}} \approx z$. χ is then given by $z_{\text{eff}}w$. These corrections to the coordination number are rather modest

because z is so high. For simulations on the ordinary cubic lattice with small coordination number, $z = 6$, more than half the interactions of each monomer are self interactions [25], and one estimates that $z_{eff} = 2.3$, for "long" chains with $N = 32$.

The weak segregation theories strictly apply only to single component block copolymers; i.e., in the absence of added solvent. To account for the presence of solvent sites in our simulations, we note that for large N, w_0 becomes small, much smaller than $w_{ow,c} \approx 0.08$, which is the value of w at the critical point for a mixture of oil and water only. For $w \ll w_{ow,c}$, the oil and water units should remain nearly uniformly dispersed. Indeed, Figure 3 shows the head and solvent composition profiles $\langle C_H(z) \rangle$ and $\langle C_w(z) \rangle$ for 60% $H_{24}T_{24}$ in the ordered state near the disordering transition. Note that the solvent compositional distribution is reasonably uniform, compared to the nonuniform head distribution. Thus, for the $H_{24}T_{24}$ system near w_0, the oil and water solvents act for the most part merely as diluents that reduce the effective number of head-tail contacts, and, following Fried and Binder [26], we can define for large N the effective χ parameter as: $\chi_{eff} \approx C_A \chi = C_A z_{eff} w$. That this definition of χ_{eff} is appropriate for $H_{24}T_{24}$ can be seen in the top half of Table 2, which shows that when C_A is increased from 0.6 to 0.8, with the oil/water ratio constant at unity, w_0 decreases so that $C_A z_{eff} w_0$ remains nearly constant. Similar behavior is observed for the disordering transition.

For smaller N and larger w_0, however, $w_0 > w_{ow,c}$, the oil and water tend to segregate with the tail head units, respectively, so that the approximation $\chi_{eff} \approx C_A \chi$ will no longer be valid. Figure 4 shows the head and water compositional profiles for 60% H_3T_3 near the disordering transition. In this case, unlike that of Figure 3, oil and water tend to segregate with heads and tails, respectively. For 60% H_3T_3, it is therefore more appropriate to define $\chi_{eff} = z_{eff} w$. That this is the more appropriate definition is

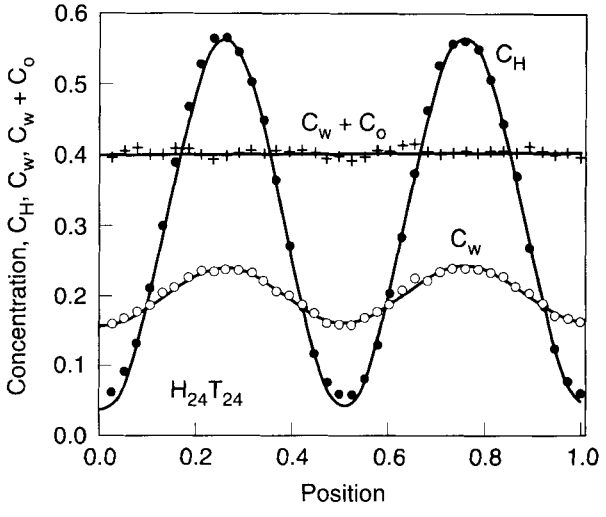

Figure 3 Composition profiles of head, water, and total solvent (water + oil) for 60% $H_{24}T_{24}$ on a 38 × 38 × 38 lattice at $w = 0.0275$, which is just above the disordering transition. The lines are sine waves fitted to these profiles whose amplitudes correspond to compositional order parameters of $S_H = 0.87$ for the amphiphile and $S_W = 0.0$ for the water.

Table 2 Lamellar transitions as a function of amphiphile concentration.

	Box size	C_A	w_0	$C_A z_{eff} N w_0$	$z_{eff} N w_0$	*Spacing d*	$d/R_{g,0}$
$H_{24}T_{24}$	38 × 38 × 38	0.6	0.0310	19.6	32.7	19	4.71
$H_{24}T_{24}$	38 × 38 × 38	0.8	0.0240	20.2	25.3	19	4.71
H_3T_3	20 × 20 × 20	0.6	0.1370	12.8	21.4	8.94	6.80
H_3T_3	20 × 20 × 20	0.8	0.1330	16.6	20.8	8.16	6.20
H_3T_3	20 × 20 × 20	0.9	0.1330	18.7	20.8	7.07	5.37

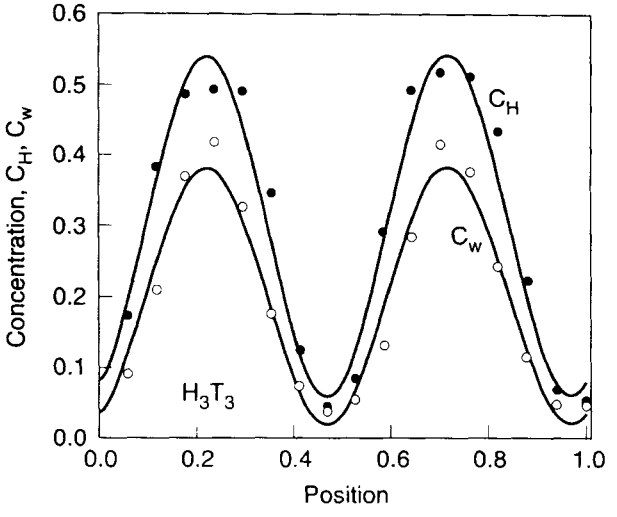

Figure 4 Head and water composition profiles for 60% H_3T_3 on a 17 × 17 × 17 lattice at $w = 0.1385$, which is just above the disordering transition. The compositional order parameters are $S_H = 0.80$ for the amphiphile, and $S_W = 0.90$ for the solvent.

supported by the bottom entries of Table 2, which show that as C_A increases toward unity, w_0 for H_3T_3 decreases only slightly. Hence $C_A z_{eff} N w_0$ increases significantly, but $z_{eff} N w_0$ remains roughly constant. Thus for small N, it is more appropriate to take $\chi_{eff,o} = z_{eff} w$, while for large N, $\chi_{eff,o} = C_A z_{eff} w_0$.

To compare the results of the simulation with the predictions of weak segregation theories, we will also need to decide which of the two transition values, w_0 or w_d, is closer to the *equilibrium* value w_{eq} at which ordering would occur in the limit of arbitrarily long equilibration times. Note in Table 1 that with increasing N, the *hysteresis* in the transition, given by $w_0/w_d - 1$, increases. This increasing hysteresis is also shown in Figure 5, which plots the average dimensionless interaction energy $\langle E \rangle$ per lattice site as a function of $C_A z_{eff} N w$ during cooling and reheating for amphiphiles of lengths 8–48. For $H_{24}T_{24}$ on a 60 × 60 × 60 lattice, w_d is about 18% lower than w_0; for H_4T_4, w_d is only 4% less than w_0. (Although the hysteretic difference, $w_0/w_d - 1$, *increases* with N, the difference in $\langle E \rangle$ between the ordered and disordered state at a given w in the hysteresis region *decreases* with N. The decreasing difference in $\langle E \rangle$

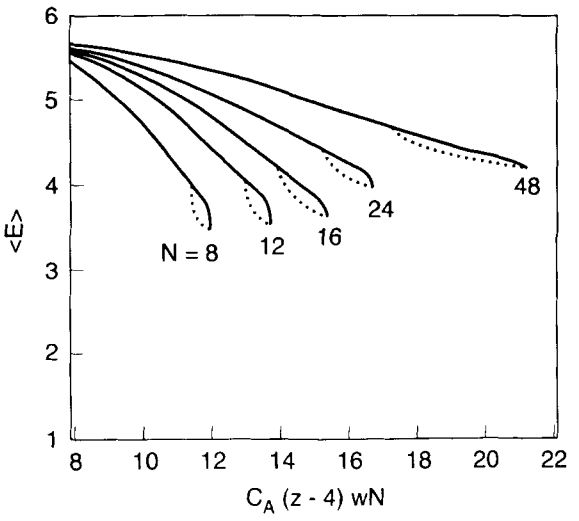

Figure 5 Average dimensions interaction energy $\langle E \rangle$ per lattice site as a function of w for 60% H_iT_i with $i = 4 - 24$. All runs were carried out on $40 \times 40 \times 40$ lattices, except for $H_{24}T_{24}$, where a $60 \times 60 \times 60$ lattice was used. The solid lines are the results for increasing w, or "cooling;" the dashed lines are for "heating." The points where the dashed line meets the solid lines mark the ordering transition on "cooling" and the disordering transition on "heating."

between disordered and ordered states at N increases is consistent with the FH and *BF* theories, which predict that the first-order transition becomes ever weaker as N increases.)

The large value of $w_0/w_d - 1$ at high N is consistent with the Fredrickson-Helfand and Barrat-Fredrickson theories, which predict that when $N \to \infty$, the *spinodal* value of w at which the disordered state becomes unstable to the ordered state on cooling should become separated infinitely far from the value of w_d. This latter result seems paradoxical, since one might expect the relative difference between w_0 and w_d to decrease as the transition becomes more weakly first order with increasing N, but for long block copolymers, a large hysteretic gap between w_0 and w_d is both predicted and experimentally observed [27, 28]. Indeed, for kinetic reasons, one observes in general that there is a greater departure from the equilibrium phase transition in "supercooling" to the ordered state than in "superheating" to the disordered phase. This general observation was confirmed also in our simulations by using especially long annealing runs for the system $H_{24}T_{24}$ on the $38 \times 38 \times 38$ lattice. It was found in these runs that w_0 could be shifted from 0.0310 to 0.0290, while w_d remained fixed at 0.0265.

In the simulations, the disordering transition occurs much faster than the ordering transition; the computer time T required for a defect-free lamellar phase to emerge from a disordered state should scale as L^5, while for the reverse process we expect $T \propto L^3$. We expect a factor of L^2 greater time for the ordering transition than the disordering transition, because in the former, a well ordered defect-free pattern is obtained by a diffusive process that eliminates all but a single direction of orientation of the lamellar domains. Thus, for a computer budget, the location of the disordering

transition can be determined for larger boxes than can the location of the ordering transition.

Notice also in Table 1 for $H_{24}T_{24}$ that w_d appears to be less sensitive to lattice size than is w_0. A systematic study of the effect of lattice size on w_d was carried out for 60% $H_{12}T_{12}$; the results appear in Table 3. Initial states for the ordered phases on large $56 \times 56 \times 56$ and $112 \times 112 \times 112$ boxes were prepared by periodic replication of the ordered phase obtained on the $28 \times 28 \times 28$ lattice. To obtain w_d, w was decreased in step sizes of 0.0010; thus the uncertainty in w_d due to the step size is large enough to account for all the variation in w_d shown in Table 3, and *no systematic effect of box size on w_d is found.*

For the reasons discussed above, the equilibrium value of the inverse dimensionless ordering temperature w_{eq} is probably much closer to w_d than to w_0, and we will compare the theoretical predictions of w_{eq} with the simulation values of w_d. However, the conclusions we draw are not much affected by the choice of w_d as opposed to w_0.

We now compare the results of the computer simulations with the predictions of the weak segregation theories. First, let us consider the lamellar spacing d at the order-disorder transition. In the absence of solvents, the weak segregation theories of Leibler [12] and of Fredrickson and Helfand [13], predict $d \to 3.2\, R_{g,0}$. Barrat and Fredrickson corrected this prediction numerically to allow for "chain-stretching" near the ordering transition; they predict a value of $d/R_{g,0}$ that increases as N decreases. Here $R_{g,0}$ is the random-flight radius of gyration of the polymer, given by the usual Gaussian formula, $R_{g,0} = b(N-1)^{1/2}/\sqrt{6}$, where b is the statistical segment length of a monomer. As discussed in section II, for our lattice model, because of the face- and body-diagonal neighbors that are allowed, the length of a segment can be 1, $\sqrt{2}$, or $\sqrt{3}$, and the average value of b^2 is 2.08. Hence, to compare our simulation results with the theory, we take $b = \sqrt{2.08} = 1.44$. With this value of b, we compute $d/R_{g,0} = \sqrt{6}d/b(N-1)^{1/2}$, from our lattice simulations, and present the results in Table 1. In the Barrat-Fredrickson theory, $d/R_{g,0}$ at the order-disorder transition is a weak function of the quantity $\bar{N}$, which for our lattice model is given by $\bar{N} = N(C_A b^3)^2 = 3.24\,\mathrm{N}$. From Figure 3 of Barrat and Fredrickson, we find $d/R_{g,0} \approx 3.8$ for $N = 48$ ($\bar{N} = 156$), which is about 20% smaller then the value $d/R_{g,0} = 4.70$ we obtain for $N = 48$. Some of this difference is caused by the presence of the solvent, which swells the radius of the coil, making it larger than the random-flight value by about 10% for $H_{24}T_{24}$ at $w = 0$. The bottom of Table 2 shows that the lamellar spacing of H_3T_3 can decrease significantly when the solvent concentration is reduced.

Figure 6 compares the values of $\chi_{\mathrm{eff},d}N$ obtained from the simulations with the theoretical values of $\chi_{\mathrm{eff}}N$ in Figure 6. Note in Figure 6 that $\chi_{\mathrm{eff},d}N \approx 18$–$21$, for

Table 3 Lattice-size dependence of w_d for 60% $H_{12}\varepsilon_{12}$, O/W = 1.

	Box size	w_d
$H_{12}T_{12}$	$28 \times 28 \times 28$	0.0490
$H_{12}T_{12}$	$35 \times 35 \times 35$	0.0495
$H_{12}T_{12}$	$40 \times 40 \times 40$	0.0485
$H_{12}T_{12}$	$56 \times 56 \times 56$	0.0490
$H_{12}T_{12}$	$112 \times 112 \times 112$	0.0490

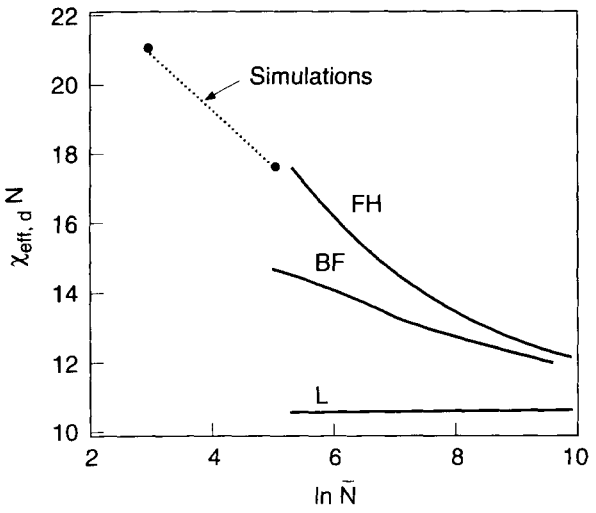

Figure 6 Predictions of Leibler (L), Fredrickson-Helfand (FH), and Barrat-Fredrickson (BF) theories for $\chi_{eff,d}N$ as a function of rescaled amphiphile length $\bar{N}$. ($\bar{N}$ equals 3.24 N for our lattice model.) Also shown are the values obtained from the simulation for H_3T_3 and $H_{24}T_{24}$.

H_3T_3 and $H_{24}T_{24}$, which is in the range expected based on the HF theory, but is rather high compared to the predictions of the more complete *BF* theory. Fried and Binder, whose simulations were carried out on a simple cubic lattice with coordination number $z = 6$, and 20% vacancies, found their values of $C_A w_0 N$ in the range 7.5–9 for $N = 16 - 60$. Using the estimate $z_{eff} \approx 2.3$ for the longer chains on this lattice gives a value $\chi_{eff,o}N = 17 - 21$, consistent with our findings. The Fredrickson-Helfand (FH) theory predicts that $\chi_{eq}N$ should depend weakly on N as $\chi_{eq}N \rightarrow 10.5 + 41\,N^{-1/3}$ for $N \rightarrow \infty$. This prediction reduces to the Leibler (L) value of $\chi_{eq}N = 10.5$ when N approaches infinity. The Barrat-Fredrickson (BF) theory predicts a smaller finite-N correction to the Leibler value than does the FH theory; see Figure 6. Although the results of the simulations accord better with the FH theory than with the more complete BF theory, neither theory can really be expected to hold at values of N as small as 48.

B Compositional order parameter

The strength of the segregation near the transition can be probed by computing the compositional order parameter S_H for the head groups. To do this, we generate ordered lamellar states on lattices whose dimension is commensurate with the preferred lamellar spacing, so that the lamellae orient parallel to a face of the lattice. The composition profile $\langle C_H(z) \rangle$ can then easily be computed as discussed in section III. These profiles for $H_{24}T_{24}$ and H_3T_3 are plotted in Figures 7 and 8 for the lamellar and the disordered states for w just above and just below w_d. Of course, in the disordered state, $\langle C_H(z) \rangle$ is uniform, except for fluctuation contributions that are not completely averaged out over the duration of the run. In the ordered state, $\langle C_H(z) \rangle$ can be fitted

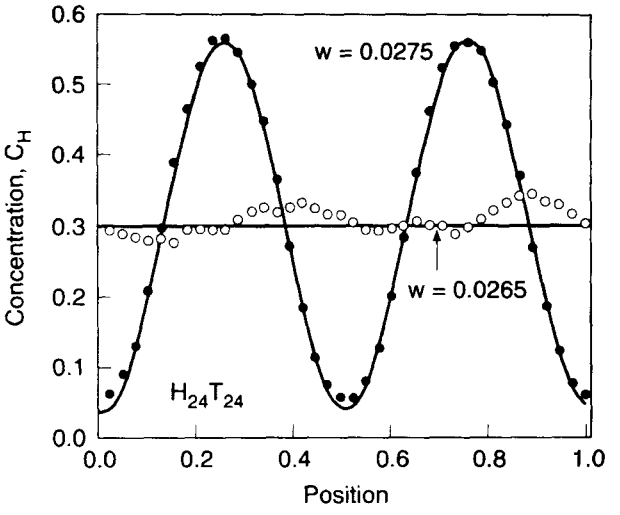

Figure 7 Head composition profiles for 60% $H_{24}T_{24}$ on a 38 × 38 × 38 lattice at $w = 0.0275$, which is just above the disordering transition, and at $w = 0.0265$, which is just below it.

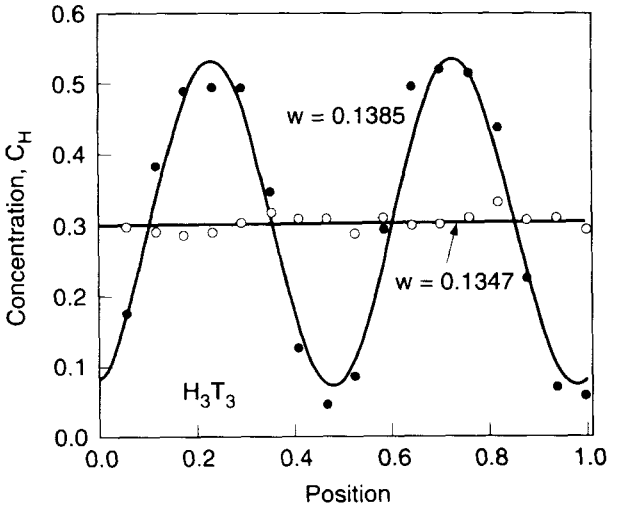

Figure 8 Head composition profiles for 60% H_3T_3 on a 17 × 17 × 17 lattice at $w = 0.1385$ just above the disordering transition, and at $w = 0.1347$, just below it.

well by a sine wave, the amplitude of which can be used to extract the compositional order parameter S_H. Since the total solvent concentration is uniform at $C_W + C_O = 0.4$ (see Figure 3), the maximum possible peak-to-peak height of the sine wave is 0.6, which is not too much greater than the actual height of 0.48 for H_3T_3 and 0.52 for $H_{24}T_{24}$. Thus $S_H = 0.48/0.60 = 0.80$ for H_3T_3, and $S_H = 0.87$ for $H_{24}T_{24}$. For 80% $H_{24}T_{24}$ at $w = 0.0200$, which is very near its disordering transition, we find $S_H = 0.66/0.8 = 0.83$;

thus the presence of solvent does not strongly affect the compositional order parameter of the amphiphile. These values for the compositional order parameter are higher than the Helfand-Fredrickson prediction that $S_H = 0.815\,\bar{N}^{-1/6}$. According to this, the order parameter should decrease from 0.56 to 0.35 as $\bar{N}$ increases from 10 to 156; but the simulations show that S_H is nearly constant at $S_H \approx 0.8$ over this range of chain lengths. Thus for chains of length 48 segments or less, the compositional order parameter predicted by weak segregation theories does not seem to be reliable.

We note that the composition profiles in the ordered state for H_3T_3 and $H_{24}T_{24}$ are not sensitive to the duration of runs used to average out fluctuations, as long as the runs are not so long that the lamellar pattern begins to drift across the simulation box. We also find that the size of the box does not strongly influence the composition profile. Figure 9 shows the composition profile for 60% $H_{12}T_{12}$ in the ordered state at $w = 0.0500$ on a $56 \times 56 \times 56$ lattice, which is large enough to contain four lamellae. As on smaller lattices, the profile is a sine wave with a large amplitude, namely 0.50, corresponding to an order parameter of 0.83.

The sinusoidal character of the profile only persists for w near w_0; at significantly larger w, the profile takes on the form expected for strongly segregated block copolymers. Figure 10 shows the profile for 60% $H_{12}T_{12}$ at $w = 2w_0 = 0.1060$ and Figure 11 shows a slice of this system on a $68 \times 68 \times 68$ lattice. At this value of w, the oil and water solvents are well segregated from each other and we estimate $\chi_{\text{eff}}N \approx (z-4)wN = 56$. Notice in Figure 10 that at this value of $\chi_{\text{eff}}N$ the profile resembles a square wave more than a sign wave, and that the gradients in head concentration are limited to well defined interfacial zones. The width t of these zones, estimated by the slope $dz/(dC_H/0.6)$ at the interface midpoint, is around 2.5–3. The strong segregation theory predicts [10] for the width $t = 2b/(6\chi_{\text{eff}})^{1/2} \approx 0.8$. The

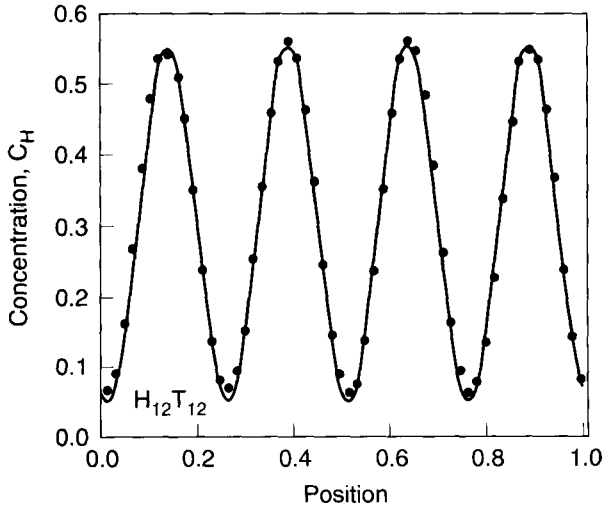

Figure 9 Head composition profiles for 60% $H_{12}T_{12}$ on a $56 \times 56 \times 56$ lattice at $w = 0.0500$, which is just above the disordering transition. The line is a sine function whose amplitude corresponds to a compositional order parameter of 0.83.

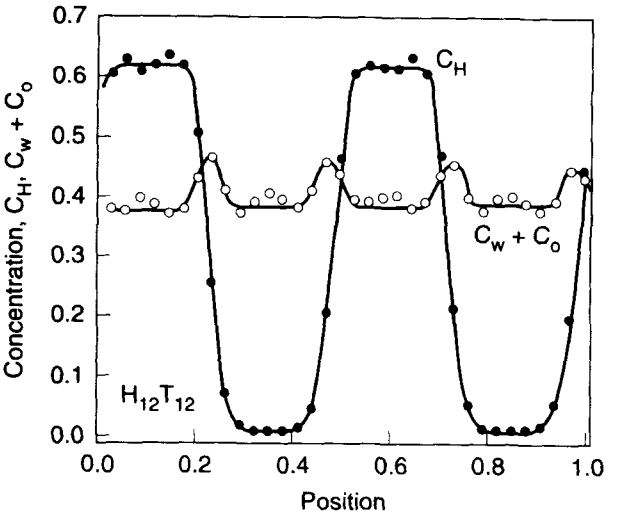

Figure 10 Composition profiles of heads and total solvent for 60% $H_{12}T_{12}$ on a 34 × 34 × 34 lattice at $w = 0.1060$, in the "strong segregation regime."

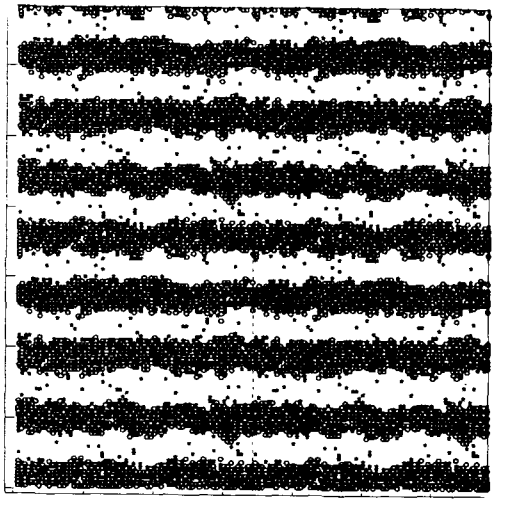

Figure 11 Slice of a 68 × 68 × 68 system containing 60% $H_{12}T_{12}$ with an oil/water ratio of unity in the strongly ordered state $w = 0.1060$.

discrepancy is not surprising since the theory fails when the interface width approaches the size of a single unit. Notice also that the solvent concentration profile is no longer uniform, but instead has concentration "spikes" in the interfacial zones. Evidently the solvent prefers to reside in interfacial regions where it can help reduce the number of unfavorable contacts between head and tail units. If a single neutral solvent, rather than oil and water, were used, we would expect an even greater tendency for solvent accumulation [29] in the interfaces.

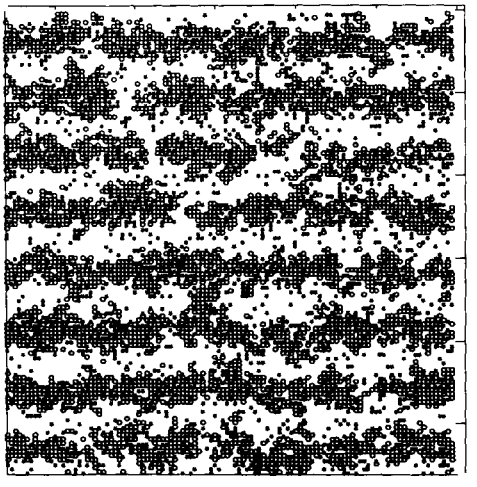

Figure 12 Slice of a 112 × 112 × 112 system contining 60% $H_{12}T_{12}$ with an oil/water ratio of unity in the ordered state $w = 0.0500$. This figure contains only one, not four, periodic images of the simulated system.

Finally, we examine qualitatively the disordering transition. Figure 12 shows 60% $H_{12}T_{12}$ on the 56 × 56 × 56 lattice at $w = 0.0500$ in the equilibrium ordered state just above the disordering transition, while Figures 13a, b show two snap-shots of the disordering that occurs when w is lowered to 0.0490. Notice that the ordered state in Figure 12 just above w_d consists of well defined lamellae, but that there are "bridge" (or "hole") defects that create channels from one head-containing or tail-containing layer to another. These defects appear and disappear spontaneously at $w = 0.0500$, but the background lamellar pattern is retained. However, when w is lowered to 0.0490, these defects accumulate as shown in Figure 13a,b, eventually leading to loss of the background lamellar pattern. Notice the difference between the moderated segregated pattern of Figure 12 and the strongly segregated pattern of Figure 11.

It is of interest to compare the discontinuous melting of lamellae in three dimensions with the continuous melting behavior of two-dimensional "stripes." Figure 14 shows the patterns formed by 80% H_4T_4 at four different values of w. As w is increased from 0.45 to 0.60, an isotropic pattern is continuously transformed by the disappearance of topological branching defects, into a pattern with anisotropy that spans the 80 × 80 box. Molten two-dimensional "stripe" phases, similar to that simulated here, have been observed in monomolecular film [30].

C Amphiphile chain statistics

In the last two sections, we found that both $\chi_{\text{eff},d}N$ and the composition order parameter near the order-disorder transition are insensitive to N for $N = 6$–48. Now, we consider the orientational order parameter, p_2, defined by equation 6, for the ordered phase close to the ordering transition. Figure 15 shows that values of p_2 computed for lamellae oriented parallel to a face of the simulation box are generally smaller than values computed for lamellae that are not parallel; i.e., there is a significant

$H_{12}T_{12}$, $C_A = 0.6$, $C_W/C_O = 1$

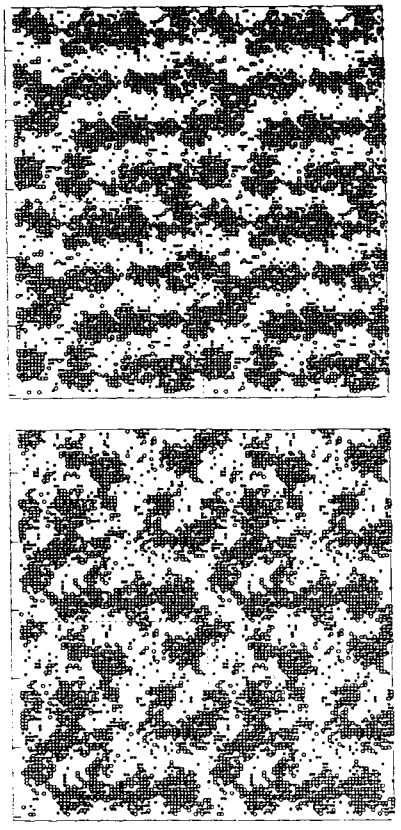

Figure 13 **a** The development of the disordered state on a 56 × 56 × 56 lattice obtained by heating the ordered state at $w = 0.0500$ to $w = 0.0490$, and annealing for 36,000 Monte Carlo steps per lattice site. **b** The same as **a** after 72,000 Monte Carlo steps per lattice site.

lattice bias effect. Furthermore, as mentioned in Section III-B, the orientation tensor for short chains is not uniaxial when the lamellae are not parallel to a face of the box. Figure 15 shows that this lattice bias effect seems to diminish with increasing N, and for $H_{24}T_{24}$, the orientation tensor is uniaxial even for lamellae not parallel to a face of the box, and p_2 is found to be nearly independent of lamellar orientation. Despite the lattice bias, the trend in Figure 15 is clear: p_2 is a rapidly decreasing function of N, going roughly as $p_2 = 1.5N^{-2}$ at high N. Thus, although for $w \approx w_0$ the compositional order parameter S_H is high and nearly independent of N, the orientational order parameter p_2 is extremely small, and rapidly decreases as the polymer molecular weight increases. This implies that unless the anisotropy in the polarizability of the blocks is very large compared to the difference in the mean polarizability between the two blocks, form birefringence will be much larger than intrinsic birefringence near the ordering transition.

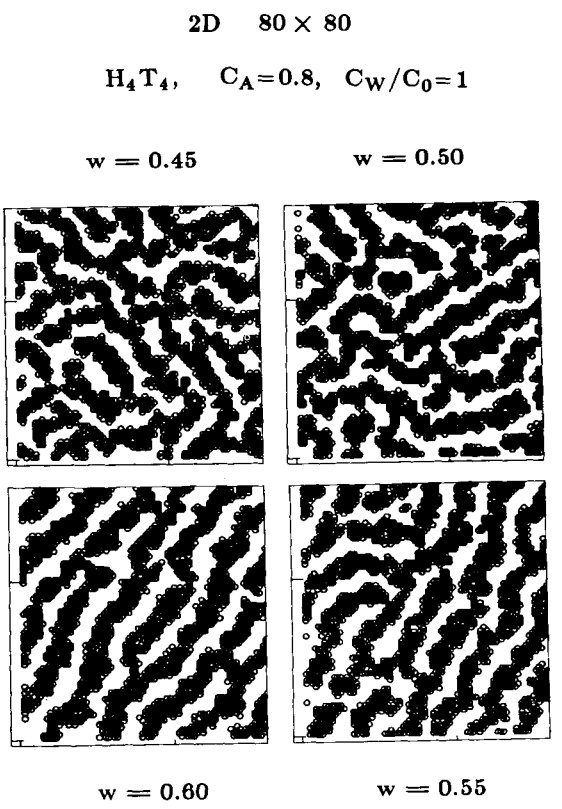

Figure 14 Two-dimensional patterns formed on 80 × 80 lattice by 80% H_4T_4 with an oil/water ratio of unity at various values of w. These contain only one, not four, periodic images of the simulated system.

From the Monte Carlo simulations, we can also compute details of the molecular configurations, in both the ordered and the disordered states. Figure 16 is a semi-log plot of $P(i^2)$ and $P_H(i_H^2)$ for 60% $H_{24}T_{24}$ in oil and water at an oil/water ratio of unity at $w = 0$ and $w = 0.0335$ in the ordered state near the transition. As defined in equation (2), $P(i^2)$ is the probability that the ends of a chain are separated by a squared distance of close to i^2 lattice cell-lengths, while $P_H(i_H^2)$ is the corresponding probability for the ends of a head group. (By symmetry $P_T(i_T^2)$ for the tail groups is the same as $P_H(i_H^2)$). Notice that the chains expand somewhat as w increases from 0 to w_0. The change in the distribution of configurations that occurs when the transition at $w = w_0$ is crossed should in principle be discontinuous, since the transition is first order, but we find that the jump is negligibly small.

For $w = 0$, we find that the mean-square separation of the chain ends, $R^2 \equiv \sum_i i^2 P(i^2)$, is 118.3. This value is somewhat larger than the random walk value, $b(N-1)^{1/2} = 97.6$, because of excluded-volume effects that are not completely screened out; thus the coil is swollen by about 10% at $w = 0$. If excluded-volume effects were absent, then P would decay exponentially with i^2; this would correspond to so-called

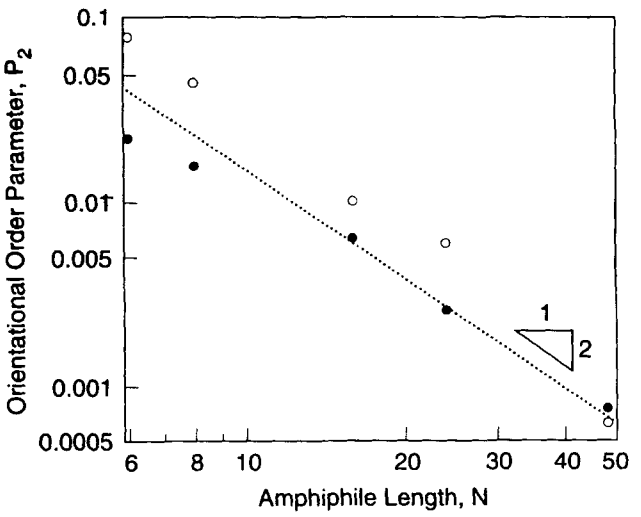

Figure 15 The orientational order parameter p_2 as a function of N in the ordered state near the order-disorder transition. The closed (open) symbols were computed on lattices in which the lamellae were parallel (not parallel) to a face of the simulation box.

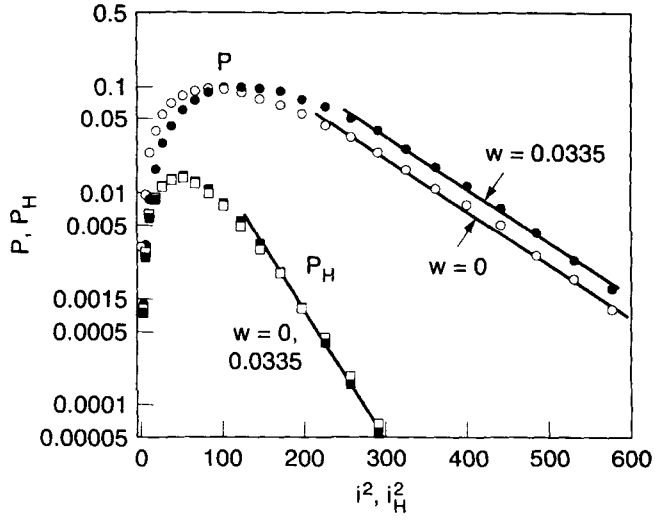

Figure 16 Probability distribution of squared separations of the ends of the $H_{24}T_{24}$ chain (P), and of the ends of the head group of $H_{24}T_{24}$ (P_H), at $w = 0$ and in the ordered state at $w = 0.0335$. The straight line segments indicate Gaussian behavior.

Gaussian behavior, which would yield a straight line on Figure 16. Note in Figure 16 that Gaussian behavior is achieved for $i^2 \gtrsim 250$, but that the densities of configurations for $i^2 < 100$ – which are relatively contracted conformations – are severely depleted because of the excluded-volume effect.

When w is increased from $w = 0$ to $w = w_0 = 0.0335$, which is just high enough to produce the ordered lamellar state, R^2 increases from 118.3 to 146.9. The conformation distribution remains Gaussian for $i^2 > 250$, but the average coil size is somewhat expanded beyond that for $w = 0$, because of the repulsive interactions between the head and tail units. Such expansion has been observed in neutron scattering experiments on diblock copolymers, and has been predicted by weak segregation theories [14].

Figure 16, which also plots P_H versus i_H^2, shows that as w increases from 0 to w_0, there is little expansion of the head or tail portions of the amphiphile, a result also predicted by the *BF* theory. The mean square separation of the ends of the head or tail groups, respectively R_H^2 or R_T^2, increase only slightly from 57.0 to 58.6 as w increases from 0 to w_0. Thus, on average, as w increases, the coil formed by the head group moves away somewhat from the coil formed by the tail group, so that R^2 increases, but the heat and tail coils themselves are barely distorted at all from their shapes at $w = 0$. Apparently it is in this way that the chains maintain maximum entropy while managing to displace head and tail units away from each other so that energetic contacts between head and tail units are significantly reduced. A similar finding was reported by Fried and Binder [26].

V SUMMARY AND DISCUSSION

By varying the length N of a symmetric amphiphile over the range 6 to 48, we have compared the disorder-to-lamellar phase transition for molecules of length typical of small-molecule surfactants to that typical of short block copolymers. We find that the critical value of $\chi_{\text{eff}}N$ at which the transition occurs is in the range 18–21. Furthermore, the one-dimensional amphiphile concentration wave in the ordered lamellar state near the transition is nearly sinusoidal, as one would expect in the weak segregation limit, yet its amplitude is high, $\gtrsim 0.8$, for all N studied. Thus, for low values of N in the range 6–48, the weakest segregation possible in an ordered lamellar state appears to be "moderate segregation"; i.e., with sinusoidal composition profiles but high order parameter.

Why is this "intermediate" level of segregation nearly independent of N over nearly a decade variation in N? As part of a speculative explanation, we note that the free energy expressions for block copolymer compositional patterns have rather sharply focused minima. This implies that compositional fluctuations with wavelength near this minimum are thermodynamically "cheap," while those far from the minimum are "expensive." In an ordered lamellar pattern, there is a fundamental wavelength, which is the lamellar spacing, plus higher harmonics. The fundamental wavelength is near the free-energy minimum, and can easily grow to large amplitude as χN increases, while the harmonics are displaced far enough away from the minimum that they are strongly suppressed, unless $\chi_{eq}N$ becomes much larger than $(\chi_{\text{eff}}N)_0$. It is amusing that in the original block copolymer theory of Helfand and coworkers, a critical value of $\chi_{eq}N \approx 20$ was estimated by extrapolating the strong segregation, or "narrow interface," approximation to the order-disorder transition. In these calculations and in our simulations, a high value of $\chi_{eq}N \approx 20$ was obtained because the blocks are well segregated at the transition; in the calculations of Helfand *et al.*, a high level of

segregation is imposed by fiat, while in the simulations it arises because of fluctuations. An important question left unresolved, however, is the value of N at which the "intermediate segregation" we observe at the ODT gives way to the weak segregation behavior predicted by the Barrat-Fredrickson theory.

Unlike the Leibler mean-field theory, which predicts that the amplitude of the lamellar pattern fades away continuously as the disordering transition is approached, our simulations depict a more violent end of the lamellar pattern in low molecular weight block copolymers. As w decreases toward w_d, fluctuations in the pattern occur, including formation of "bridge" or "hole" defects. For $w > w_d$, these fluctuations come and go, and the locally disrupted pattern always relaxes back toward the stationary lamellar pattern. But at $w = w_d$, the defects apparently become numerous enough to interfere with the relaxation process. A given distortion wants to relax, but may relax toward the wrong pattern because of interfering patterns created by other defects. The result, at $w = w_d$, is a catastrophic growth in the density of defects, until the lamellar pattern is ripped apart. This picture is akin to that of the melting of simple crystalline solids, which occurs when the amplitude of fluctuations in the crystal reach a value given by the Lindemann criterion [31].

The presence of rapidly fluctuating equilibrium "bridge" defects in the ordered phase near the transition might provide a means for much more rapid diffusion of block copolymer chains across lamellae than would be possible by diffusion of single chains across the "mean field" compositional pattern. Thus the fluctuating bridge defects might help account for experimental data showing little change in molecular diffusivity when the order-disorder transition is crossed [32, 33]. Also, the presence of "bridge" defects might affect the shear properties of block copolymers, since bridges would tend to keep the lamellae from sliding readily past each other, if the shear rate is higher than the rate of formation and destruction of these bridges. It has been shown that near the ordering transition lamellar block copolymers under shear can orient with the lamellae orthogonal to the shearing surfaces [23, 34]. Perhaps this orthogonal orientation occurs because it minimizes the straining of "bridges" between lamellae.

Acknowledgement

I appreciate the helpful comments of Gene Helfand.

References

[1] E. L. Thomas, D. B. Alward, D. J. Kinning, D. C. Martin, D. L. Handlin Jr. and L. J. Fetters, "Ordered bicontinuous double-diamond structure of star bleok copolymers: A new equilibrium microdomain morpology", *Macromolecules*, **19**, 2197 (1986).

[2] H. Hasegawa, K. Tanaka, K. Yamasaki and T. Hashimoto, "Bicontinuous microdomain morphology of block copolymers. 1. Tetrapod-network structure of polystyrene-polyisoprene diblock polymers", *Macromolecules*, **20**, 1651 (1987).

[3] K. Almdal, K. A. Koppi, F. S. Bates and K. Mortensen, "Multiple ordered phases in a block copolymer melt", *Macromolecules*, **25**, 1743 (1992).

[4] P. Kekicheff and B. Cabane, "Between cylinders and bilayers: Structures of intermediate mesophases of the SDS/water system", *J. Phys.* (Paris) **48**, 1571 (1987).

[5] P. Kekicheff and G. J. T. Tiddy, "Structure of the intermediate phase and its transformation to lamellar phase in the lithium perfluorooctanoate/water system", *J. Phys. Chem.*, **93**, 2520 (1989).

[6] H. Hagslätt, O. Söderman and B. Jönsson, "The structure of intermediate ribbon phases in surfactant systems", *Liquid Crystals*, **12**, 667 (1992).
[7] V. Luzzati and P. A. Spegt, "Polymorphism of lipids", *Nature*, **215**, 701 (1967).
[8] S. M. Gruner, "Stability of lyotropic phases with curved interfaces", *J. Phys. Chem.*, **93**, 7562, (1989).
[9] K. Winey, E. L. Thomas and L. Fetters, " Isothermal morphology diagrams for binary blends of diblock copolymer and homopolymer", *Macromolecules*, **25**, 2645 (1992).
[10] E. Helfand, "Block copolymer theory. III Statistical mechanics of the microdomain structure", *Macromolecules*, **8**, 552 (1975); E. Helfand and Z. R. Wasserman, "Block copolymer theory. 4. Narrow interphase approximation", *Macromolecules*, **9**, 879 (1976).
[11] A. N. Semenov, "Contribution to the theory of microphase layering in block-copolymer melts", *Sov. Phys. JETP*, **61**, 733 (1985).
[12] L. Leibler, "Theory of microphase separation in block copolymers", *Macromolecules*, **13**, 1602 (1980).
[13] G. H. Fredrickson and E. Helfand, "Fluctuation effects in the theory of microphase separation in block copolymers", *J. Chem. Phys.*, **87**, 697 (1987).
[14] J.-L. Barrat and G. H. Fredrickson, "Collective and single-chain correlations near the block copolymer order-disorder transition", *J. Chem. Phys.*, **95**, 1281 (1991).
[15] Z. G. Wang and S. A. Safran, "Equilibrium emulsification of polymer blends by diblock copolymers", *J. Phys.* (Paris), submitted (1990).
[16] L. Leibler, "Emulsifying effects of block copolymers in incompatible polymers blends", *Makromol. Chem. Macromol. Symp.*, **16**, 1 (1988).
[17] M. Olvera de la Cruz, "Transitions to periodic structures in block copolymer melts", *Phys. Rev. Lett.*, **67**, 85 (1991).
[18] S. A. Brazovskii, "Phase transition of an isotropic system to a nonuniform state", *Sov. Phys. JEPT*, **41**, 85 (1975).
[19] R. G. Larson, "Monte Carlo simulation of amphiphilic systems in two and three dimensions", *J. Chem. Phys.*, **89**, 1642 (1988); "Self-assembly of surfactant liquid crystalline phases by Monte Carlo simulation", **91**, 2479 (1989); "Monte Carlo simulation of microstructural transitions in surfactant systems", **92**, 7904 (1992).
[20] R. G. Larson, "Molecular simulation of ordered amphiphilic phases", *Chem. Eng. Sci.*, in press (1994).
[21] P. J. Flory, *Statistical Mechanics of Chain Molecules*, John Wiley & Sons New York, 1969.
[22] S. H. Anastasiadis, G. Fytas, S. Vogt and E. W. Fischer, "Breathing and composition pattern relaxation in "homogeneous" diblock copolymers", *Phys. Rev. Lett.*, **70**, 2415 (1993).
[23] R. G. Larson, K. I. Winey, S. S. Patel, H. Watanabe and R. Bruinsma, "the rheology of layered liquids: lamellar block copolymers and smectic liquid crystals", *Rheol. Acta*, **32**, 245 (1993).
[24] K. I. Winey, S. S. Patel, R. G. Larson and H. Watanabe, "Interdependence of shear deformations and block copolymer morphology", *Marcromolecules*, **26**, 2542 (1993).
[25] A. Sariban and K. Binder, "Monte Carlo simulation of a lattice model for ternary polymer mixtures", *Coll. Polym. Sci.*, **266**, 389 (1988).
[26] H. Fried and K. Binder, "The microphase separation transition in symmetric diblock copolymer melts: A Monte Carlo study", *J. Chem. Phys.*, **94**, 8349 (1991).
[27] K. Almdal, F. S. Bates and K. Mortensen, "Multiple ordered in a block copolymer melt", *J. Chem. Phys.*, **96**, 9122 (1992).
[28] K.A. Koppi, M. Tirrell and F. S. Bates, "Shear-induced isotropic-to-lamellar transition", *Phys. Rev. Lett.*, **70**, 1449 (1993).
[29] G. H. Fredrickson and L. Leibler, "Theory of block copolymer solutions: Nonselective good solvents", *Macromolecules*, **22**, 1238 (1989).
[30] M. Seul and M. J. Sammon, "Competing interactions and domain-shape instabilities in a monomolecular film at an air-water interface", *Phys. Rev. Lett.*, **64**, 1903 (1990).
[31] H. Kleinert, *Gauge Fields in Condensed Matter*, p. 878, World Scientific Publishing Co., London (1989).
[32] N. P. Balsara, C. E. Eastman, M. D. Foster, T. P. Lodge and M. Tirrell, "Diffusion in microstructured block copolymer solutions", *Makromol. Chem. Macromol. Symp.*, **45**, 213 (1991).
[33] G. Fleischer, F. Fujara and B. Stühn, "Restricted diffusion in the regime of the order-to-disorder transition in diblock copolymers: A field gradient NMR study", *Macromolecules*, **26**, 2340 (1993).
[34] K. A. Koppi, M. Tirrell, F. S. Bates, K. Almdal and R. H. Colby, "Lamellae orientation in dynamically sheared diblock copolymer melts", *J. Phys.* (Paris) 2, 1941 (1993).